

Consensus-based Communication-aware Formation Control for a Mobile Multi-agent System

Sang Xing

*Department of Mathematics
and Statistics
Portland State University
Portland, OR 97201
sxing@pdx.edu*

Thomas Yang

*Department of Electrical Engineering
and Computer Science
Embry-Riddle Aeronautical University
Daytona Beach, FL 32114
Tianyu.Yang@erau.edu*

Houbing Song

*Department of Electrical Engineering
and Computer Science
Embry-Riddle Aeronautical University
Daytona Beach, FL 32114
h.song@ieee.org*

Abstract—Over the past few decades, unmanned aerial vehicle (UAV) technology has played a significant role in military and civilian applications. To meet the challenges of the future, in addition to improving the functionality and utility of individual aircraft, there is a need to consider how to develop more effective UAV management and organizations. Consequently, among the many developments in UAVs, formation control has become an important concept in recent years. Formation control requires multiple UAVs to adapt to the mission including generate a formation, stay in formation, and change formation. In this paper, we further constrain the formation controller model, not only estimate the desired separation with acceptable accuracy but also ensure a consensus among estimates. Thus, optimizes the overall communication performance of a dynamical multi-agent system.

Index Terms—Unmanned Aerial Vehicles, Multi-agent Systems, Communication-aware, Decentralized, Distributed, Consensus-based,, Formation Control

I. INTRODUCTION

Due to the limited equipment can be carried by a single UAV, it is necessary to send out multiple missions to complete a more complex task. A swarm of UAVs operating in formation can disperse equipment, split a complex task into several simple tasks, and assign them to different UAVs in the formation, which will perform the task more efficiently.

Multiple UAVs can carry different equipment and collaborate to accomplish tasks that cannot be accomplished by a single UAV, such as high-precision positioning, multi-angle imaging and theater communication relay. In classical formation control, agents typically perceive their absolute position relative to the global coordinate system, and by actively control agents' absolute positions to achieve their desired formation [1]. Communications between agents are usually assumed to be ideal within a certain range of communication [2].

In this paper, we adopted ideas from [3], where author Li constructs a communication-aware formation controller that uses the communication channel quality, which is measured locally by agents to guide agents into a desired formation. Thus, it also optimizes the overall communication quality of the formation system.

Inspired by [4], where the motion of each individual aircraft, better known as agent, is imposed of kinematic unicycle model with constraints on its airspeed and travel direction. We

further constrains the communication-aware formation control to reach a consensus between any pair of connected agents. The formation system is shown in Fig. 1. We first have an interaction model at the communication layer, which takes the agents' position as input and outputs agents' relative position with respect to their neighboring agents. The coordinates of this set of relative positions are then taken as the input for our control layer. A gradient-based controller is imposed at the control layer, where the communication quality among agents are reached at its maximum performance. We then have our second controller, the consensus controller,that manages all agents' relative positions at the control layer, and outputs the final control of agents with consensus of all agents traveling in the desired direction.

The remainder of the paper are organized as follows. In Section II, we describe the preparatory work in order to understand the formation control process of a dynamical multi-agent system. Section III presents the derivation of interaction model at the communication layer. These two controllers construct a final formation controller model, which is presented in Section IV.Simulation results are delivered in Section V. Lastly, we concludes the paper in Section VI.

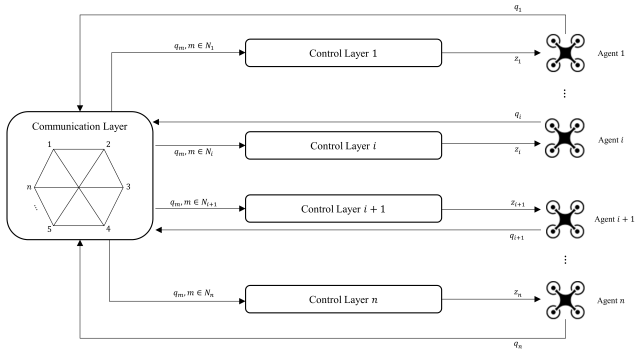


Fig. 1. Schematic diagram of distance-based formation control

II. PRELIMINARIES

A. System Model

Consider the following n single-integrator modeled agents in a two-dimensional space, given by

$$\dot{q}_i = z_i, \quad i = 1, 2, \dots, n, \quad (1)$$

where $q_i, z_i \in \mathbb{R}^2$, $q, z \in \mathbb{R}^{2n}$, and $i \in \mathcal{V}, \mathcal{V} = \{1, 2, \dots, n\}$,

- q_i denotes the *position input* of i -th agent.
- z_i denotes the *control input* of i -th agent.
- The *formation set* is denoted as $q = \{q_1^\top, q_2^\top, \dots, q_n^\top\}^\top$.
- The *control set* is denoted as $z = \{z_1^\top, z_2^\top, \dots, z_n^\top\}^\top$.

B. Graph Theory

A graph G is a pair of $(\mathcal{V}, \mathcal{E})$ consisting of a set of *vertices* $\mathcal{V} = \{1, 2, \dots, n\}$ and a set of ordered pairs of the vertices $\mathcal{E} \subseteq \mathcal{V} \times \mathcal{V}$, called *edges*. I.e., $\mathcal{E} = \{(i, j) \mid i, j \in \mathcal{V}, j \neq i\}$. Here, we assume that there is no self-edge, i.e., $(i, i) \notin \mathcal{E}$.

The graph G is said to be *strongly connected* if there is a path from any node to the other nodes. The graph G is said to be *undirected* if $(i, j) \in \mathcal{E} \Leftrightarrow (j, i) \in \mathcal{E}$. The length of any two vertices in a connected graph is no larger than $n - 1$.

The set of *neighbors* of agent $i \in \mathcal{V}$ is defined as a set $N_i = \{j \in \mathcal{V} : (i, j) \in \mathcal{E}\}$.

C. Rigid Formation

Many researchers have investigated the distributed control of rigid body formation using artificial potential fields [5]. Among these researchers, many have studied the distributed control of rigid formations by adapting ideas from the theory of graph rigidity. The formation of groups of mobile agents in which all inter-agent distances remain constant is called *rigid* [6]. Agents sense relative positions of their neighbors with respect to their own local coordinate systems. To be specific, the relative position vector between agent i and agent j is denoted as $\vec{q}_{ij} = q_i - q_j$ [7], and the relative distance between agent i and agent j is denoted as

$$r_{ij} = \sqrt{(x_i - x_j)^2 + (y_i - y_j)^2} = \|q_i - q_j\|. \quad (2)$$

Let $R > 0$ denote the *communication range* between two agents. In a two-dimensional open ball with radius R (see Fig. 2.), the neighboring set of agent i can be denoted by

$$N_i = \{j \in \mathcal{V} \mid r_{ij} \leq R\}. \quad (3)$$

D. Control Gain Matrices

Consider a group of n nonholonomic agents performing formation mission in a two-dimensional plane. We denote $q_i = [x_i, y_i]^\top \in \mathbb{R}^2$ as the position input of agent i in a common global coordinate frame, and u_i as the consensus control law, that we define as

$$u_i = \sum_{j \in N_i} A_{ij}(q)(q_i - q_j), \quad (4)$$

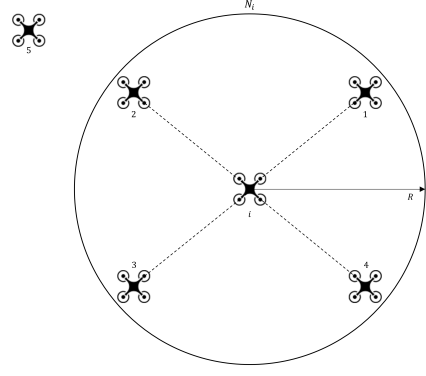


Fig. 2. Agent i and its neighbors in a circle neighborhood

where $A_{ij} \in \mathbb{R}^{2 \times 2}$ are constant *control gain matrices* constrained in the form

$$A_{ij} = \begin{bmatrix} a_{ij} & b_{ij} \\ -b_{ij} & a_{ij} \end{bmatrix}, \quad a_{ij}, b_{ij} \in \mathbb{R}. \quad (5)$$

Author in [8] showed that the dynamics between q_i and q_j that are expressed in the agents' local coordinate frame is the same as in the case of coordinates expressed in a common global frame. Therefore, while the consensus formation control is distributed and uses local relative position sensing each others, the consensus control can be designed and analyzed in a global coordinate frame. The geometric intuition behind the control strategy (4) is explained in [4].

Consequently, the consensus control for all agents in the closed-loop dynamics can be expressed as

$$u = \{u_1^\top, u_2^\top, \dots, u_n^\top\}^\top \in \mathbb{R}^{2n}, \quad (6)$$

where

$$u = Aq, \quad (7)$$

and

$$A = \begin{bmatrix} -\sum_{j=2}^n A_{1j} & A_{12} & \cdots & A_{1n} \\ A_{21} & -\sum_{j=1, j \neq 2}^n A_{2j} & \cdots & A_{2n} \\ \vdots & \vdots & \ddots & \vdots \\ A_{n1} & A_{n2} & \cdots & -\sum_{j=1}^{n-1} A_{nj} \end{bmatrix} \quad (8)$$

is the aggregate state matrix in $\mathbb{R}^{2n \times 2n}$ that consists of A_{ij} 's, and Laplacian matrix structure. For $j \notin N_i$, then $A_{ij} = 0$ in (8). From the Laplacian matrix structure of A , it follows that

$$\begin{aligned} \mathbf{1} &:= [1, 0, 1, 0, \dots, 1, 0]^\top \in \mathbb{R}^{2n} \\ \bar{\mathbf{1}} &:= [0, 1, 0, 1, \dots, 0, 1]^\top \in \mathbb{R}^{2n} \end{aligned} \quad (9)$$

are in the kernel of A [4].

Let $q^* \in \mathbb{R}^{2n}$ denote the positions of agents in any embedding of the desired formation. Furthermore, let $\bar{q}^* \in \mathbb{R}^{2n}$ denote the coordinates of agent in this embedding when the formation is rotated by 90 degrees around the origin.

It has been demonstrated in [8], that the agent will converge to the intended formation by rotating, translating, and non-negative scaling factors regardless of their initial condition

from which the formation starts, if A satisfies the following two conditions

- Vectors $\mathbf{1}$, $\bar{\mathbf{1}}$, q^* and \bar{q}^* are in the kernel of A ,
- Other than the four zero eigenvalues associated with these eigenvectors, the remaining eigenvalues of A have negative real parts.

We then design a stabilizing gain matrix that meets these two conditions listed above. Define

$$B := [q^*, \bar{q}^*, \mathbf{1}, \bar{\mathbf{1}}] \in \mathbb{R}^{2n \times 4}, \quad (10)$$

where $\mathbf{1}, \bar{\mathbf{1}}$ are given in (9). Since B is a set of bases for the kernel of A , we let $USV^\top = B$ be the singular value decomposition (SVD) of B , where

$$U = [\bar{Q}, Q] \in \mathbb{R}^{2n \times 2n}, \quad (11)$$

with $Q \in \mathbb{R}^{2n \times (2n-4)}$ defined as the last $2n - 4$ columns of U . Using Q in (11), we define

$$\bar{A} = Q^\top A Q \in \mathbb{R}^{(2n-4) \times (2n-4)}, \quad (12)$$

to show that matrices A and \bar{A} have the same set of nonzero eigenvalues.

According to what has been observed, U is an orthogonal matrix, and $\text{range}(\bar{Q}) = \text{range}(B)$. The projection of A onto the orthogonal complement of $\text{range}(B)$ is hence \bar{A} . The projection (12) removes the zero eigenvalues of A effectively, enable us to describe the stability of A in terms of \bar{A} .

For an undirected sensing topology, matrix A can be designed to be symmetric. In this case, \bar{A} is symmetric, and its eigenvalues are real and sortable. As a result, A can be computed by solving the following semi-definite programming (SDP) problem

$$\begin{aligned} A &= \underset{a_{ij}, b_{ij}, \gamma}{\text{argmax}} && \gamma \\ &\text{subject to} && \bar{A} + \gamma I \preceq 0 \\ &&& AB = 0 \end{aligned} \quad (13)$$

where the initial constraint is a linear matrix inequality. Once control gain matrices are computed, they can be sent to agents prior to the mission. Without requiring complete understanding of the sensor topology, (13) can be solved via a distributed optimization technique [10]. In recent years, effective algorithms for numerically solving SDPs have been developed and are now available [11]–[13]. The proposed Algorithm 1 provides a summary of the suggested method for determining stabilizing gain matrix A and consensus control u .

III. COMMUNICATION LAYER

In the communication layer, two different communication models are presented to measure the signal qualities as it propagates through space in the antenna near-field and far-field. In addition, for comprehensive consideration, a communication-aware interaction model is used to illustrate the signal propagation in the near and far-fields of the antenna.

Algorithm 1 Finding A and u

Data: B // Bases of $\ker(A)$
 q // Coordinates of Agents
 u // Consensus Control

Result: Control gain matrix A . Consensus control u .

for $B = (10)$ **do**

$U = [U, \sim, \sim] = \text{SVD}(B);$
 $Q = U(:, 1:2n-4);$
 $\bar{A} = Q^\top A^* Q;$
 $A = \text{SDP}(\bar{A})$ s.t. satisfies (13);
 $u = A^* q$

end

A. Antenna Far-field Propagation

In a mobile ad hoc network, the quality of communication services depends on many unknown parameters besides relative positions, such as multipath finding, shadowing, noise, and interference [14]. The *outage probability* is introduced as an important wireless channel metric when analyzing the channel quality. The outage probability is defined as the probability that the instantaneous Signal-to-Noise Ratio (SNR) is below a certain threshold [15],

$$P_{\text{out}} = 1 - \exp\left(-\alpha(2^\delta - 1)\left(\frac{r}{r_0}\right)^v\right), \quad (14)$$

where α is a system parameter about antenna characteristics, δ is the required application data rate, v is the path loss exponent that changes depending on the physical environment, r_0 is a reference distance that divides the antenna near-field and far-field, and r is the Euclidean distance between a transmitter and a receiver. It is intuitive to see that as r grows, the outage probability $P_{\text{out}} \rightarrow 1$ and, as $r \rightarrow 0$, $P_{\text{out}} \rightarrow 0$ in (14).

Then the *reception probability* of a single input single output (SISO) communication link is defined as

$$P_{\text{recep}} = 1 - P_{\text{out}} = \exp\left(-\alpha(2^\delta - 1)\left(\frac{r}{r_0}\right)^v\right). \quad (15)$$

The likelihood that the receiver will accurately receive information from the transmitter is assessed by the reception probability (15). The reception probability models the quality of the communication link a_{ij} between agent i and agent j in the antenna's far field:

$$a_{ij} = \exp\left(-\alpha(2^\delta - 1)\left(\frac{r_{ij}}{r_0}\right)^v\right) = \exp\left(-\beta\left(\frac{r_{ij}}{r_0}\right)^v\right), \quad (16)$$

where $\beta = \alpha(2^\delta - 1)$, and α , δ , v , and r_0 are all fixed parameters.

The channel quality (16) is inversely proportional to the inter-agent distance r_{ij} . When the distance between agents

is far apart, the reception probability may fall below a certain threshold, which means that the communication between agents becomes unreliable. To some extent, the communication range is similar to the reception probability threshold, where inter-agent distances are no longer within the communication range, leading to edge disappearance and message loss. As a corollary, we bridge the two conceptual ideas between the communication channel model and the graph topology model.

The set of neighbors of agent i is now defined as

$$N_i = \{j \in \mathcal{V} \mid a_{ij} \geq P_T\}, \quad (17)$$

where P_T is a reception probability threshold. Agents discards the incoming packets when the reception probability is less than P_T .

B. Antenna Near-field Propagation

The antenna near-field is a region that is close to the antenna. The boundary between antenna near-field and antenna far-field is vaguely defined by the reference distance r_0 [16]. Since the signal propagation in the near-field region of the antenna is quite complex, it is usually difficult to obtain an accurate antenna near-field communication model. For the general tradeoff, we design to use a simple approximate model to capture the signal propagation in the antenna near-field denoted by [15]

$$g_{ij} = \frac{r_{ij}}{\sqrt{r_{ij}^2 + r_0^2}}. \quad (18)$$

It can be concluded from (18), as $r_{ij} \rightarrow 0$, the channel quality $g_{ij} \rightarrow 0$, which characterizes the interference effect in the antenna near-field; while when r_{ij}/r_0 , $g_{ij} \rightarrow 1$, suggesting that the interference effect can be disregarded in the antenna far-field.

C. Communication-aware Interaction Model

As a matter of fact, signals suffers from the signal scattering effect, interference effect and path loss effect in both antenna regions. Therefore, it is necessary to fully consider both two propagations when designing a communication interaction model. Thus, the communication-aware interaction mode is designed as follows [3]:

$$\phi(r_{ij}) = g_{ij} \cdot a_{ij} = \frac{r_{ij}}{\sqrt{r_{ij}^2 + r_0^2}} \cdot \exp\left(-\beta\left(\frac{r_{ij}}{r_0}\right)^v\right). \quad (19)$$

From (19), we want to find a distance r_{ij}^* , that brings the optimal inter-agent communication. Due to the path loss effect and signal scattering effect, any value that is larger or smaller than r_{ij}^* distance will result in inadequate communication performance. Therefore, we apply the first-order derivative to (19), to find the maximum of communication performance. We denote the first order derivative of (19) with respect to r_{ij} as

$$\frac{d\phi}{dr_{ij}} = \varphi(r_{ij}), \quad (20)$$

where

$$\varphi(r_{ij}) = \frac{-\beta v(r_{ij})^{v+2} - \beta v r_0^2 (r_{ij})^v + r_0^{v+2}}{\sqrt{(r_{ij}^2 + r_0^2)^3}} \cdot \exp\left(-\beta\left(\frac{r_{ij}}{r_0}\right)^v\right). \quad (21)$$

From (21), we know that both $\sqrt{(r_{ij}^2 + r_0^2)^3}$ and $\exp(-\beta(r_{ij}/r_0)^v)$ are greater than 0 for all $r_{ij} \in [0, \infty)$. So whether $\phi(r_{ij})$ has a maximum or not is totally determined by the function

$$f(r_{ij}) = -\beta v(r_{ij})^{v+2} - \beta v r_0^2 (r_{ij})^v + r_0^{v+2}. \quad (22)$$

Let $f(r_{ij}) = 0$, the maximum is obtained at

$$r_{ij}^* = \frac{r_0}{(\beta v)^{\frac{1}{v}}}. \quad (23)$$

Moreover,

$$\begin{cases} \varphi(r_{ij}) > 0, & \forall r_{ij} \in [0, r_{ij}^*], \\ \varphi(r_{ij}) = 0, & \forall r_{ij} = r_{ij}^*, \\ \varphi(r_{ij}) < 0, & \forall r_{ij} \in (r_{ij}^*, \infty), \end{cases} \quad (24)$$

which means the interaction model $\phi(r_{ij})$ reaches its maximum performance denoted by ϕ^* at r_{ij}^* given in (23).

IV. CONTROL LAYER

In the control layer, distributed controllers are designed for each mobile agent using the local state and states from the neighbors. Each controller consists of two terms: gradient term and consensus term. By adapting the concept of artificial potential field, the gradient-based controller ensures agents within the communication range R , form and maintain the ideal formation for optimal communication performance. Meanwhile, the consensus controller ensures that eventually all agents will be traveling in one direction over time for a common goal.

A. Artificial Potential Propagation

An artificial potential function $\psi(r_{ij})$ between agent i and agent j is defined to have the following properties [3]:

- 1) $\psi(r_{ij})$ is a nonnegative function of r_{ij} ,
- 2) $\psi(r_{ij})$ is continuously differentiable,
- 3) $\psi(r_{ij})$ reaches its strict minimum at $r_{ij} = r_\alpha$, i.e., $\psi(r_{ij})$ and $\psi(r_{ij}) > 0$ for all $r_{ij} \neq r_\alpha$.

The potential function $\psi(r_{ij})$ encrypts a rigid formation with a desired distance r_α . A gradient-based control law is a distributed rigid formation control that can be designed as the negative gradient of its local potential functions

$$\mathcal{G}_i = -\nabla_{q_i} \left[\sum_{j \in N_i} \psi(r_{ij}) \right]. \quad (25)$$

We define a pairwise potential function to evaluate the interaction between any pairs of agents regardless of whether they are neighbors or not by

$$\psi_t(r_{ij}) = \begin{cases} \psi(r_{ij}), & \forall (i, j) \in \mathcal{E}, \\ \psi(R) & \text{otherwise.} \end{cases} \quad (26)$$

For $r_{ij} \geq R$, the potential function $\psi_t(r_{ij})$ remains constant, indicating that when edge (i, j) is lost, agents i and agent j

will no longer influence each other any more. It is important to keep in mind that $\psi_t(r_{ij})$ is not always differentiable at the transition point of $r_{ij} = R$,

Let $\psi_t(r_{ij})$ be an attractive or repulsive pairwise potential with a global minimum at r_{ij} and a finite cut-off at R . Then, the *collective potential function* of the formation group can be denoted as

$$W(q) = \frac{1}{2} \sum_{i=1}^n \sum_{j=1}^n \psi_t(r_{ij}). \quad (27)$$

The right-hand side of the potential function $W(q)$ might not be smooth when the topology changes.

B. Gradient Controller

Inspired by the ideas of artificial potential fields, the gradient-based controller can be further designed for agents to converge in the desired formation with optimal communication performance. It is written as

$$\begin{aligned} \mathcal{G}_i &= -\nabla_{q_i} \left[\sum_{j \in N_i} \psi_t(r_{ij}) \right] \\ &= \nabla_{q_i} \left[\sum_{j \in N_i} \phi(r_{ij}) \right] \\ &= \sum_{j \in N_i} \left[\nabla_{q_i} \phi(r_{ij}) \right] \\ &= \sum_{j \in N_i} \left[\varphi(r_{ij}) \cdot e_{ij} \right], \end{aligned} \quad (28)$$

where $e_{ij} = (q_i - q_j)/r_{ij}$. For faster convergence, e_{ij} can be written as $(q_i - q_j)/\sqrt{1 + kr_{ij}}$, where $k \in (0, 1)$.

C. Unicycle Kinematic Model with Dubins Constraints

Now that we have achieved a desired formation with optimal neighboring communication, our last objectives is to allow this group of dynamic agents to travel at the same direction. A distributed consensus control scheme is proposed to drive all n agents to a formation in which the agents develops same directional velocity vector over time, and thus optimizes network coverage. Assume that the airspeed and heading angle of a UAV are adjusted to desired values. We denote $q_i = [x_i, y_i]^\top \in \mathbb{R}^2$ as the position input of agent i in the X - Y frame as illustrated in Fig. 3. The unicycle kinematic model of agent i is represented by:

$$\begin{aligned} \dot{x}_i &= \nu_i \cos(\theta_i) \\ \dot{y}_i &= \nu_i \sin(\theta_i) \\ \dot{\theta}_i &= \omega_i, \end{aligned} \quad (29)$$

The unicycle kinematic model provides a good description of the UAV's motion at a constant altitude [4]. In Fig. 3, $x_i, y_i \in \mathbb{R}$ are coordinates of agent i . The agent's heading vector h_i makes an angle θ_i with respect to x -axis, where $\theta_i \in [0, 2\pi]$. ρ_{ij} represents the line of sight angle between agent i and j with $\rho_{ij} = \arctan 2(q_i - q_j)$. $\nu_i \in \mathbb{R}$ is the linear velocity vector and $\omega_i \in \mathbb{R}$ is respectively the angular velocity vector of the UAV. Scalars ν_i and ω_i are defined as

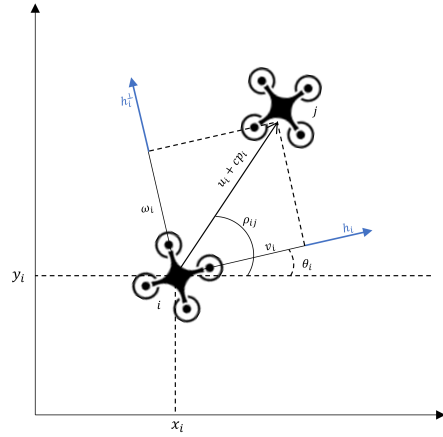


Fig. 3. Close-loop Dynamic with Dubins Constraints

the projections of the consensus control vector $u_i + cp_i$. u_i was previously defined in (4). $c > 0$ is a constant desired speed. $p_i \in \mathbb{R}^2$ is the constant unit vector that the agent i should travel along to reach the desired destination.

The UAV's airspeed and heading angle are constrained by its physical limitations. The Dubins constraints can be used to represent these physical bounds in real-world simulations,

$$\begin{aligned} \nu_{\min} &\leq \nu_i \leq \nu_{\max}, \\ |\omega_i| &\leq \omega_{\max}, \end{aligned} \quad (30)$$

where $\nu_{\max} > \nu_{\min} > 0$ and $\omega_{\max} > 0$ are positive real scalars. Input constraints (30), together with the kinematic model (29), are referred as the Unicycle Kinematic Model with Dubins Constraints. Although this model is ideally suited for high level path planning and path tracking control design, it is not accurate enough for low level autopilot design because it does not account for aerodynamics, wind effects, disturbances, etc.

D. Consensus Controller

We define the heading vector $h_i \in \mathbb{R}^2$ and its perpendicular vector $h_i^\perp \in \mathbb{R}^2$ as follows to develop an alternate formulation for (29) that is more appropriate for the formation control design.

$$h_i := \begin{bmatrix} \cos(\theta_i) \\ \sin(\theta_i) \end{bmatrix}, \quad h_i^\perp := \begin{bmatrix} -\sin(\theta_i) \\ \cos(\theta_i) \end{bmatrix}. \quad (31)$$

The motion of agent i can be expressed by

$$\begin{aligned} c_i &= h_i \nu_i \\ \dot{h}_i &= h_i^\perp \omega_i, \end{aligned} \quad (32)$$

Let $q \in \mathbb{R}^{2n}$ and $h \in \mathbb{R}^{2n}$ be the aggregate position input vector and aggregate heading vectors of all agents respectively. Let $\nu \in \mathbb{R}^n$ and $\omega \in \mathbb{R}^n$ be the aggregate linear velocity, and aggregate angular velocity vectors, respectively. This notation can be used to describe the motion of all agents as

$$\begin{aligned} \mathcal{C} &= H\nu \\ \dot{h} &= H^\perp \omega, \end{aligned} \quad (33)$$

where matrices $H, H^\perp \in \mathbb{R}^{2n \times n}$ are defined as

$$H = \begin{bmatrix} h_1 & 0 & \cdots & 0 \\ 0 & h_2 & & 0 \\ \vdots & \ddots & \vdots & \\ 0 & 0 & \cdots & h_n \end{bmatrix}, \quad H^\perp = \begin{bmatrix} h_1^\perp & 0 & \cdots & 0 \\ 0 & h_2^\perp & & 0 \\ \vdots & & \ddots & \vdots \\ 0 & 0 & \cdots & h_n^\perp \end{bmatrix}. \quad (34)$$

Consider a team of UAVs with control (33). We attempt to assign guidance ν and ω to agents so that they fly autonomously towards the same desired destination.

The proposed consensus control strategy for a multi-agent system is as follows. The control vector for each agent is calculated as $u_i + cp_i$, which then can be projected onto the heading vector h_i and its perpendicular vector h_i^\perp . The linear and angular velocity vectors now can be written in terms of h_i and h_i^\perp . Specifically, the linear and angular velocity controls are given by

$$\begin{aligned} \nu_i &= h_i^\top (u + cp_i) \cos(\rho_{ij} - \theta_i) \\ \omega_i &= h_i^{\perp\top} (u + cp_i) \sin(\rho_{ij} - \theta_i) \end{aligned} \quad (35)$$

The control for all agents can be expressed collectively in the vector form as

$$\begin{aligned} \nu &= H^\top (u + cp) \cos(\rho - \theta) \\ \omega &= H^{\perp\top} (u + cp) \sin(\rho - \theta) \end{aligned} \quad (36)$$

where H and H^\perp are defined in (34). Under the proposed control, the consensus dynamics are given by replacing (35) in (32) as

$$\begin{aligned} \mathcal{C}_i &= h_i h_i^\top (u + cp_i) \cos(\rho_{ij} - \theta_i) \\ \dot{h}_i &= h_i^\perp h_i^{\perp\top} (u + cp_i) \sin(\rho_{ij} - \theta_i), \end{aligned} \quad (37)$$

and collectively

$$\begin{aligned} \mathcal{C} &= HH^\top (u + cp) \cos(\rho - \theta) \\ \dot{h} &= H^\perp H^{\perp\top} (u + cp) \sin(\rho - \theta). \end{aligned} \quad (38)$$

E. Constrained Formation Controller

Finally, the dynamics of this multi-agent system thus can be expressed by the sum of gradient-based control and consensus control where

$$\begin{aligned} \dot{q}_i &= z_i \\ &= \sum_{j \in N_i} \underbrace{[\varphi(r_{ij}) \cdot e_{ij}]}_{\text{gradient-based term}} + \sum_{j \in N_i} \underbrace{[A_{ij}(q)(q_i - q_j)]}_{\text{consensus term}} \\ &= \sum_{j \in N_i} \underbrace{[\varphi(r_{ij}) \cdot e_{ij}]}_{\text{gradient-based term}} + \sum_{j \in N_i} \underbrace{[h_i h_i^\top (u + cp_i) \cos(\rho_{ij} - \theta_i)]}_{\text{consensus term}} \\ &= \mathcal{G}_i + \mathcal{C}_i. \end{aligned} \quad (39)$$

V. SIMULATION AND EVALUATION

In this section, we provide a few simulation to illustrate our proposed formation control method. The parameters of our simulations are listed in the following table. The position input of agents are chosen randomly in a static environment. The desired formation is implemented using Algorithm 2.

TABLE I
SIMULATION PARAMETERS

Parameter	Value
α	1×10^{-5}
δ	2
v	3
r_0	5
P_T	94%

Algorithm 2 Proposed Formation Control Algorithm

Data: $itr \leftarrow 1000$ // Number of Iterations
 $n \leftarrow 8$ // Number of Agents
 $J \leftarrow N_i$ // Number of Neighbors
 a_{ij} // Communication Near-field Model
 $P_T \leftarrow 0.94$ // Reception Threshold
 φ_{ij} // Interaction Model
 \mathcal{G}_i // Gradient-term Controller
 \mathcal{C}_i // Consensus-term Controller
 \dot{q} // Dynamics of Multi-agent System

Result: Desired Swarm Formation Control (see Fig. 4.)

```

for 1 :  $itr$  do
  for 1 :  $n$  do
    for  $J = N_i ; a_{ij} = (16)$  do
      if  $a_{ij} \geq P_T$  then
        |  $\varphi(r_{ij}) = (21);$ 
      else
        |  $\varphi(r_{ij}) = 0;$ 
      end
    end
  end
   $\mathcal{G}_i = (28);$ 
   $\mathcal{C}_i = (37);$ 
   $\dot{q} = \mathcal{G}_i + \mathcal{C}_i$ 
end

```

Consider a group of 8 agents using the communication setting specified in the above table. The initial topology of 8 agents in the given communication environment is displayed in Fig. 5(a), where the initial positions of 8 agents are given by $x_1 = [-5, -14]^\top$, $x_2 = [-5, -19]^\top$, $x_3 = [0, 0]^\top$, $x_4 = [20, 21]^\top$, $x_5 = [35, 41]^\top$, $x_6 = [68, 0]^\top$, $x_7 = [72, 13]^\top$, $x_8 = [72, -18]^\top$.

The circular nodes represents individual agents. The blue lines represents the communication links. The red arrows represents the directional vectors of each agent.

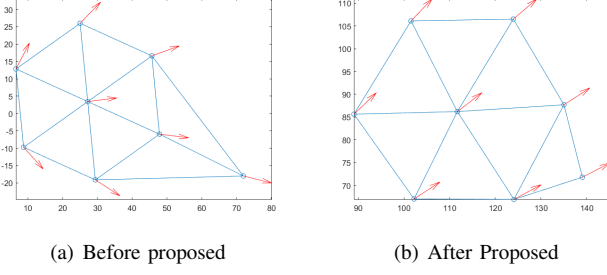


Fig. 4. Multi-agent system before and after our proposed formation control algorithm

Fig. 4(a) shows the result of 8 agents before our proposed control (39). Fig. 4(b) shows that after our proposed implementation, all the agents are able to walk along the same direction and approach to each other in a desired formation.

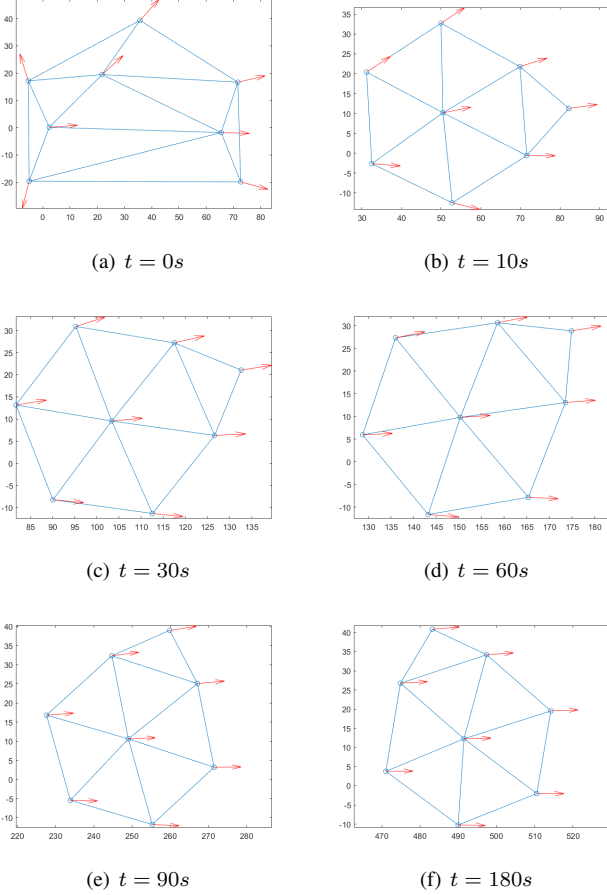


Fig. 5. Simulation of 8 UAVs starting from random initial pose and achieving an optimal formation while traveling along toward the positive x -axis.

Fig. 5 provides another simulation result where all agents eventually reaches a consensus and travels in the positive x -axis direction over time.

Here, a performance index is introduced to demonstrate how a trade-off distance between agents is necessary to get the best communication performance. The average neighboring

distance r_n and average communication performance J_n are defined as

$$r_n = \frac{\sum_{i=1}^n \sum_{j \in N_i} r_{ij}}{2n|N_i|}, \quad (40)$$

$$J_n = \frac{\sum_{i=1}^n \sum_{j \in N_i} \phi(r_{ij})}{2n|N_i|}, \quad (41)$$

where $|N_i|$ represents the size of neighbors of agent i .

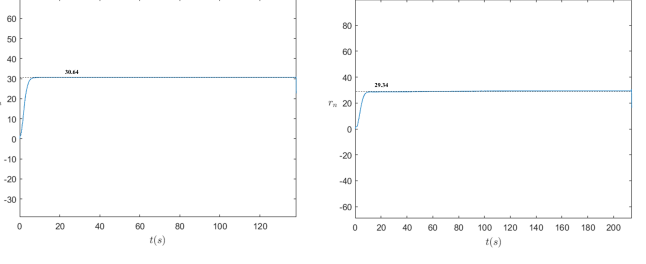


Fig. 6. Average Neighboring Distance Indicator for Agents Traveling at E direction

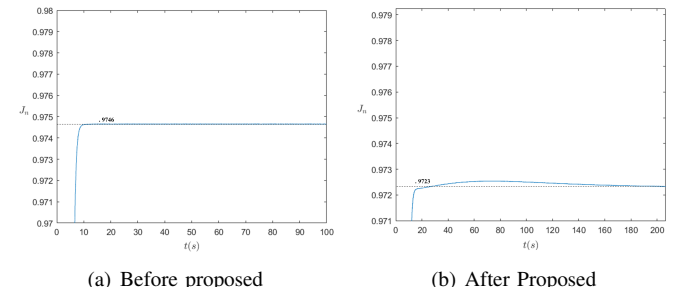


Fig. 7. Average Communication Performance Indicator for Agents Traveling at E direction

Fig. 6 showed that our proposed method was able to bring agents closer to each other. Fig. 7 shows that the communication performance of our proposed method is slightly lower compared to the original control strategy. Therefore, our proposed technique is specially suitable for applications in which it is desirable to keep agents close while achieving decent inter-agent communication performance.

VI. CONCLUSION

In this paper, we propose a new distributed formation control strategy for multi-agent systems, in which communication constraints were taken into consideration to achieve desired formations with optimal communication performance. Consensus control is also successfully enforced for a set of agents traveling in the same direction toward a desired destination. Compared to similar techniques in the literature (e.g. [3]), our proposed method strikes a balance between two distinct objectives: keeping small inter-agent distances and maintaining effective inter-agent communications.

ACKNOWLEDGMENT

This research was supported by the National Science Foundation under Grant No. 2150213.

REFERENCES

- [1] K.-K. Oh, M.-C. Park, and H.-S. Ahn, "A survey of multi-agent formation control," *Automatica*, vol. 53, pp. 424-440, Mar. 2015.
- [2] Y. Yan and Y. Mostofi, "Robotic Router Formation in Realistic Communication Environments," in *IEEE Transactions on Robotics*, vol. 28, no. 4, pp. 810-827, Aug. 2012.
- [3] H. Li, J. Peng, W. Liu, K. Gao, and Z. Huang, "A novel communication-aware formation control strategy for dynamical multi-agent systems," *Journal of the Franklin Institute*, vol. 352, no. 9, pp. 3701-3715, Sep. 2015.
- [4] K. Fathian, T. H. Summers, and N. R. Gans, "Distributed formation control and navigation of fixed-wing UAVs at constant altitude," in *2018 International Conference on Unmanned Aircraft Systems (ICUAS)*, 2018.
- [5] A. Durniak, "Welcome to IEEE Xplore," *IEEE power eng. rev.*, vol. 20, no. 11, p. 12, 2000.
- [6] J. Baillieul and P. J. Antsaklis, "Control and communication challenges in networked real-time systems," *Proc. IEEE Inst. Electr. Electron. Eng.*, vol. 95, no. 1, pp. 9-28, 2007.
- [7] R. Olfati-Saber, "Flocking for multi-agent dynamic systems: algorithms and theory," *IEEE Transactions on Automatic Control*, vol. 51, no. 3, pp. 401-420, Mar. 2006.
- [8] K. Fathian, D. I. Rachinskii, T. H. Summers, M. W. Spong, and N. R. Gans, "Distributed formation control under arbitrarily changing topology," in *2017 American Control Conference (ACC)*, 2017.
- [9] S. Boyd, "Convex optimization of graph Laplacian eigenvalues," in *Proceedings of the International Congress of Mathematicians Madrid, August 22-30, 2006, Zuerich, Switzerland: European Mathematical Society Publishing House*, 2009, pp. 1311-1319.
- [10] Z. Lin, L. Wang, Z. Chen, M. Fu, and Z. Han, "Necessary and sufficient graphical conditions for affine formation control," *IEEE Trans. Automat. Contr.*, vol. 61, no. 10, pp. 2877-2891, 2016.
- [11] Tütüncü, H. Reha, K. C. Toh, and M. J. Todd, "Solving semidefinite-quadratic-linear programs using SDPT3," *Math. Program.*, vol. 95, no. 2, pp. 189-217, 2003.
- [12] M. J. Todd, K. C. Toh, and R. H. Tütüncü, "On the Nesterov-Todd Direction in Semidefinite Programming," *SIAM J. Optim.*, vol. 8, no. 3, pp. 769-796, 1998.
- [13] K. C. Toh, M. J. Todd, and R. H. Tütüncü, "SDPT3 — A Matlab software package for semidefinite programming, Version 1.3," *Optim. Methods Softw.*, vol. 11, no. 1-4, pp. 545-581, 1999.
- [14] C. Li, Z. Qu, and M. A. Weitnauer, "Distributed extremum seeking and formation control for nonholonomic mobile network," *Systems Control Letters*, vol. 75, pp. 27-34, Jan. 2015.
- [15] A. Goldsmith, *Wireless Communications*. Cambridge, England: Cambridge University Press, 2012.
- [16] H. Li, J. Peng, X. Zhang, and Z. Huang, "Flocking of Mobile Agents Using a New Interaction Model: A Cyber-Physical Perspective," *IEEE Access*, vol. 5, pp. 2665-2675, 2017.